NACA

RESEARCH MEMORANDUM

HIGH-SPEED WIND-TUNNEL TESTS OF A $\frac{1}{16}$-SCALE MODEL OF THE D-558 RESEARCH AIRPLANE

D-558-1 SPEED-REDUCTION BRAKE AND SYMMETRICAL-PROFILE WING CHARACTERISTICS

By

John B. Wright

Langley Memorial Aeronautical Laboratory
Langley Field, Va.

NATIONAL ADVISORY COMMITTEE FOR AERONAUTICS

WASHINGTON

June 15, 1948

NATIONAL ADVISORY COMMITTEE FOR AERONAUTICS

RESEARCH MEMORANDUM

HIGH-SPEED WIND-TUNNEL TESTS OF A $\frac{1}{16}$-SCALE MODEL OF THE D-558 RESEARCH AIRPLANE

D-558-1 SPEED-REDUCTION BRAKE AND SYMMETRICAL-PROFILE WING CHARACTERISTICS

By John B. Wright

SUMMARY

The present paper contains the results of pitching-moment, lift, and drag measurements with a $\frac{1}{16}$-scale model of the D-558-1 with speed-reduction brakes and with a wing of symmetrical profile. Tests were conducted through a Mach number range up to 0.96 in the Langley 8-foot high-speed tunnel. In order to expedite this information, only a limited analysis is presented.

It was found that drag increases caused by the brakes produce a small decrement in terminal Mach number. No serious adverse longitudinal-stability changes were noted.

From tests with the model without brakes using a wing with NACA 65-010 sections, it is indicated that the adverse stability characteristics which were found with a wing of NACA 65-110 sections were not improved by the use of the symmetrical-profile wing.

INTRODUCTION

The D-558-1 is a research airplane designed to investigate aerodynamic phenomena in the transonic speed range. It is designed to fly at a level-flight Mach number of 0.85 and is powered by a turbojet unit. It has an unswept wing of aspect ratio 4.17 in a low position on the fuselage.

Wind-tunnel tests of a $\frac{1}{16}$-scale model were conducted up to high Mach numbers in the Langley 8-foot high-speed tunnel in order to provide preflight information for the pilot to insure against any catastrophic events due to compressibility effects during flight. Speed-reduction brakes on the fuselage sides are contemplated for the purpose of rapid speed reduction if adverse regions are encountered at high speeds.

The present paper gives lift, pitching-moment, and drag results from an internal-balance system with a $\frac{1}{16}$-scale model of the D-558-1 with no nose-inlet flow. This is the third in a series of papers providing longitudinal-force-characteristic information on the D-558 project. Reference 1 contains lift and drag characteristics of several different plan forms, whereas reference 2 contains longitudinal-stability characteristics of the D-558-1. Tests, reported herein, were made of the model with speed-reduction brakes fully deflected, and of the model with a wing of symmetrical profile (NACA 65-010 sections). The latter investigation was made in an attempt to reduce or eliminate instability at a Mach number of 0.9 at low lift coefficients first reported in reference 2. In order to expedite this information to the NACA flight-test group at Muroc, Calif.; to the manufacturer, Douglas Aircraft Company; and to the Bureau of Aeronautics, Department of the Navy, this paper contains only the results available at the present time with a limited analysis.

APPARATUS AND TECHNIQUE

The D-558 investigation was conducted in the Langley 8-foot high-speed tunnel, which is a single-return, closed-throat type. The maximum corrected test Mach number was approximately 0.96 for this investigation. The Reynolds number varied from about 1.0×10^6 to 1.6×10^6, based on a wing mean aerodynamic chord of 4.656 inches.

Model.- An all-metal $\frac{1}{16}$-scale model of the D-558-1 airplane was constructed by the NACA. The general layout is shown by the three-view drawing in figure 1. The geometry and dimensions of the wing and tail are given in table I. A second wing of symmetrical profile (NACA 65-010 sections) was constructed with the same area, aspect ratio, incidence, and so forth, as the standard (NACA 65-110 sections) wing. Speed-reduction brakes were mounted on each side of the fuselage for some of the tests as shown in figure 2. Since no inlet flow was simulated, the nose inlet was faired forward to form a solid nose. The fuselage was hollow to allow for the internal balance.

Model support and balance.- The sting-strut support system used in these tests is shown in figure 3. The sting, containing the balance within the fuselage, was attached to the fuselage inside and well forward. The sting diameter is smaller than the inside diameter of the fuselage so that all aerodynamic forces are transmitted through the balance. The sting enlarges smoothly aft of the model to the angle-of-attack coupling, thence to the support strut. In an attempt to avoid choking the tunnel at the strut location at a low test-section Mach number, a liner to constrict the flow was installed in the throat of the tunnel and designed to obtain the highest possible test Mach numbers at the model location.

The balance consisted of strain-gage elements located on the sting and on component parts of the sting so as to measure pitching moment, normal force, and axial force. A transferral of forces to the airplane center of gravity was required because the pitching moment was found at the center of the pitching-moment-gage location, which is a small distance from the center of gravity. In addition, the normal force and axial force had to be reoriented to the lift and drag directions by simple trigonometry.

Because of the interference of the sting on the model, two types of tare runs were made for several configurations to evaluate this interference. The tare-measuring arrangement is shown in figures 3 and 4. The tare setup incorporated auxiliary tare arms which had 6-percent airfoils sweptback 30° in forward portions to minimize high-speed interference effects. The arms were attached in the model to an internal balance similar to that used with the sting for the normal runs.

Corrections.- All data were referred to a center-of-gravity location of 25 percent mean aerodynamic chord shown in figure 1. The data were corrected for angle-of-attack changes due to bending of the sting and strain-gage-balance beams by determining the angle at each test point and interpolating to obtain constant angle of attack. The effect of temperature on the strain gages was determined in static-load and temperature tests. The temperature of the gages was measured during each run and the corresponding corrections found in static tests applied.

The data have all been corrected for the interference of the sting by measuring this effect by the two types of tare runs shown in figure 4. It was found that the sting produced an interference which decreased the pitching-moment coefficient on the average of 0.020 over the Mach number and angle-of-attack range. The interference of the sting on lift coefficient was negligible, and on drag coefficient was approximately 0.006.

The data are presented to a corrected Mach number of about 0.96. Choking occurred at the strut at this maximum test-section Mach number. The data are unaffected by choke phenomena as the strut is well aft of the model, and tunnel calibration measurements indicated no irregularities in the model test section.

Corrections for wind-tunnel effects have been applied to these data in the manner indicated in references 1 and 2.

RESULTS AND DISCUSSION

Speed-Reduction Brakes

Stability and control.- Figure 5 shows the variation of lift coefficient and pitching-moment coefficient with Mach number for constant angles of attack for the complete model with speed-reduction brakes deflected and with a tail incidence $i_t = 2.2^{\circ}$ and an elevator deflection $\delta_e = 0^{\circ}$. Figure 6 is a cross plot from figure 5 which shows the variation of pitching-moment coefficient with lift coefficient for various Mach numbers. Also shown for comparison in figure 6 is the variation for the model with the same tail settings but without the speed-reduction brake (reference 2). It is indicated that for this one tail setting the static longitudinal stability of the airplane is not appreciably changed when the brakes are extended. The tendency towards instability near a Mach number of 0.9 is less intense and appears to be extended to a smaller and lower lift-coefficient range by the brakes. It is also indicated that a small increase in the lift coefficient at $C_m = 0$ occurs. The magnitude of these effects may be modified at other tail settings.

Drag.- Figure 7 shows the variation of drag coefficient with Mach number for constant angles of attack for the complete model with speed-reduction brakes deflected. By subtracting the drag of the airplane without the brakes but with the same tail settings (reference 2) from the data in figure 7, the incremental drag due to the brakes was determined. The variation of the incremental drag with Mach number is shown in figure 8 for several angles of attack. Some decrease occurs at the high angles of attack with increasing Mach number; but, in general, an incremental-drag coefficient of approximately 0.030 to 0.025 is maintained through the highest test Mach number.

Terminal Mach number determination for the airplane at $C_L = 0$ and a wing loading of 58 pounds per square foot with and without the brakes extended is shown in figure 9. The terminal Mach numbers shown in figure 10 for various altitudes indicate the brakes can only produce approximately a 0.05 Mach number decrement at low altitudes. This decrement becomes smaller at higher altitudes and fails to limit the airplane to Mach numbers below which serious adverse stability characteristics occur. The time required at an altitude of 20,000 feet to decelerate from the terminal Mach number without the brakes (0.96) to that with the brakes extended (0.916) was calculated from the drag increase alone to be about 5 seconds.

NACA 65-010 Wing

The variation of lift and pitching-moment coefficients with Mach number for the complete model with the wing of symmetrical profile are presented in figure 11. The tail was set with $i_t = 2.2^{\circ}$ and $\delta_e = 0^{\circ}$. Figure 12 shows the variation of pitching-moment coefficient with lift coefficient for several Mach numbers. The data for the configuration with the standard (NACA 65-110 sections) cambered wing (reference 2) is shown for comparison. In general, it is indicated that similar changes in stability will occur with the uncambered wing as with the cambered wing with small changes in the lift coefficient for $C_m = 0$. It should be noted that this tail setting does not represent a high-speed trim value. It is believed however, that the trends shown here are indicative of the general effect of using a wing of symmetrical profile, even though the magnitude of the effects may differ at other conditions.

Because no tests were made with the tail removed or with more than one tail setting, details such as downwash, wing-alone characteristics, and control effects are not available. However, it can be seen that the stability characteristics at this one tail setting were not appreciably changed or improved by the use of the wing of symmetrical profile.

CONCLUDING REMARKS

From tests of a $\frac{1}{16}$-scale model of the D-558-1 airplane with no nose-inlet flow and with speed-reduction brakes deflected, it is indicated that only a small decrement in terminal Mach number is produced. No serious adverse longitudinal-stability changes were noted.

From tests with the model using a wing with an NACA 65-010 section, it is indicated that the adverse stability characteristics which were found with a wing of NACA 65-110 sections are not likely to be improved by the use of the symmetrical profile wing.

Langley Memorial Aeronautical Laboratory
National Advisory Committee for Aeronautics
Langley Field, Va.

REFERENCES

1. Wright, John B., and Loving, Donald L.: High-Speed Wind-Tunnel Tests of a 1/16-Scale Model of the D-558 Research Airplane. Lift and Drag Characteristics of the D-558-1 and Various Wing and Tail Configurations. NACA RM No. L6J09, 1946.

2. Wright, John B.: High-Speed Wind-Tunnel Tests of a $\frac{1}{16}$-Scale Model of the D-558 Research Airplane. Basic Longitudinal Stability of the D-558-1. NACA RM No. L7K24, 1947.

TABLE I

WING AND TAIL DIMENSIONS OF $\frac{1}{16}$-SCALE D-558-1 MODEL

Wing section	NACA 65-110
Wing aspect ratio	4.17
Wing taper ratio	0.54
Wing span, in.	18.76
Wing area, sq ft	0.587
Wing mean aerodynamic chord, in.	4.656
Wing incidence angle, deg	2.0
Wing dihedral, deg	4.0
Wing sweep angle (50-percent chord), deg	0
Wing-root chord, in.	5.88
Wing-tip chord, in.	3.17
Longitudinal location of 25-percent mean-aerodynamic-chord point from nose-inlet station, in. (also center-of-gravity location)	11.96
Tail section	NACA 65-008
Tail aspect ratio	4.17
Tail taper ratio	0.55
Tail span, in.	9.18
Tail area, sq ft	0.140
Tail dihedral, deg	0
Elevator area, percent of tail area	25

CONFIDENTIAL

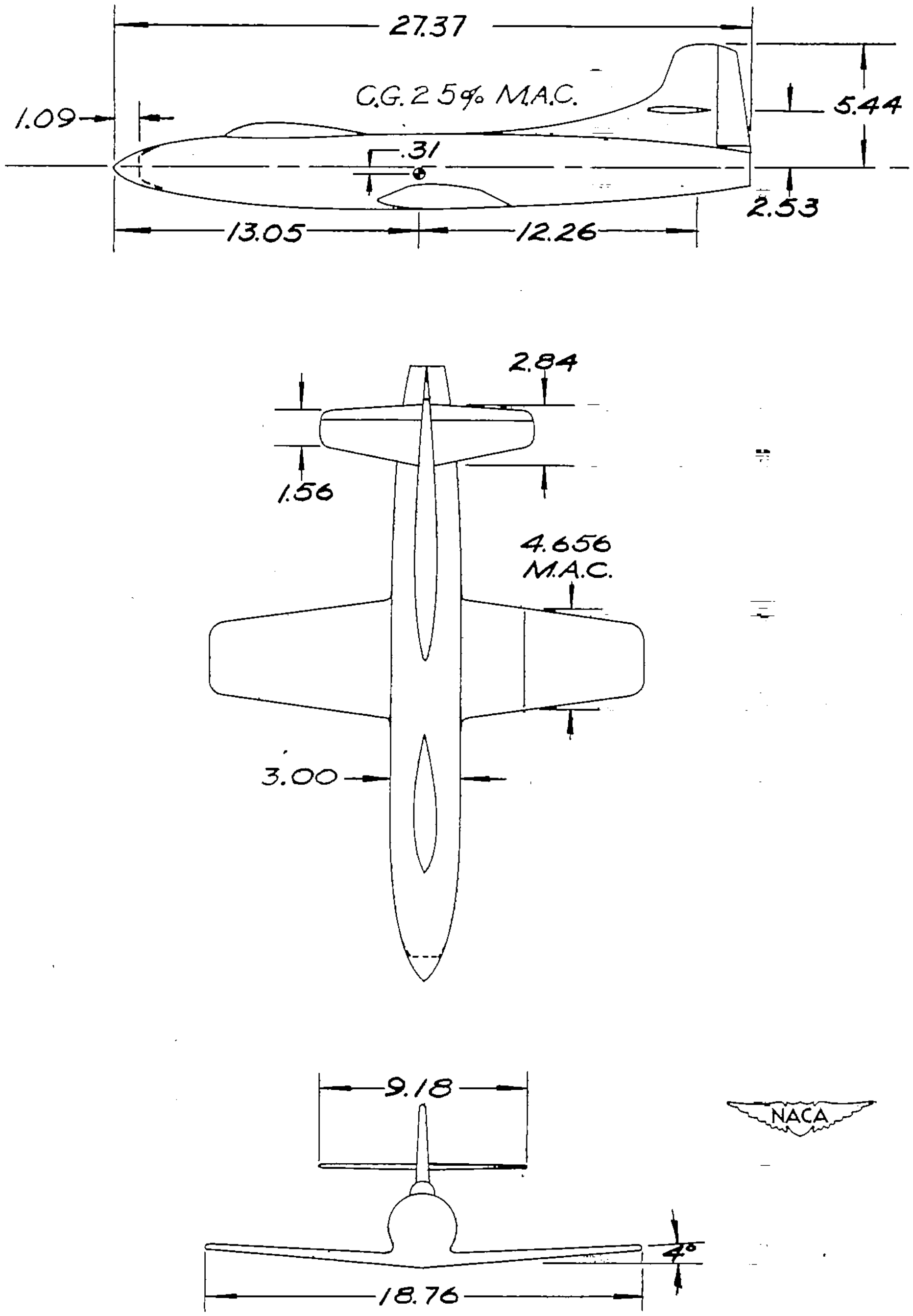

CONFIDENTIAL

Figure 1.– Drawing of 1/16-scale D-558-1 model as tested in the Langley 8-foot high-speed tunnel. All dimensions in inches.

CONFIDENTIAL

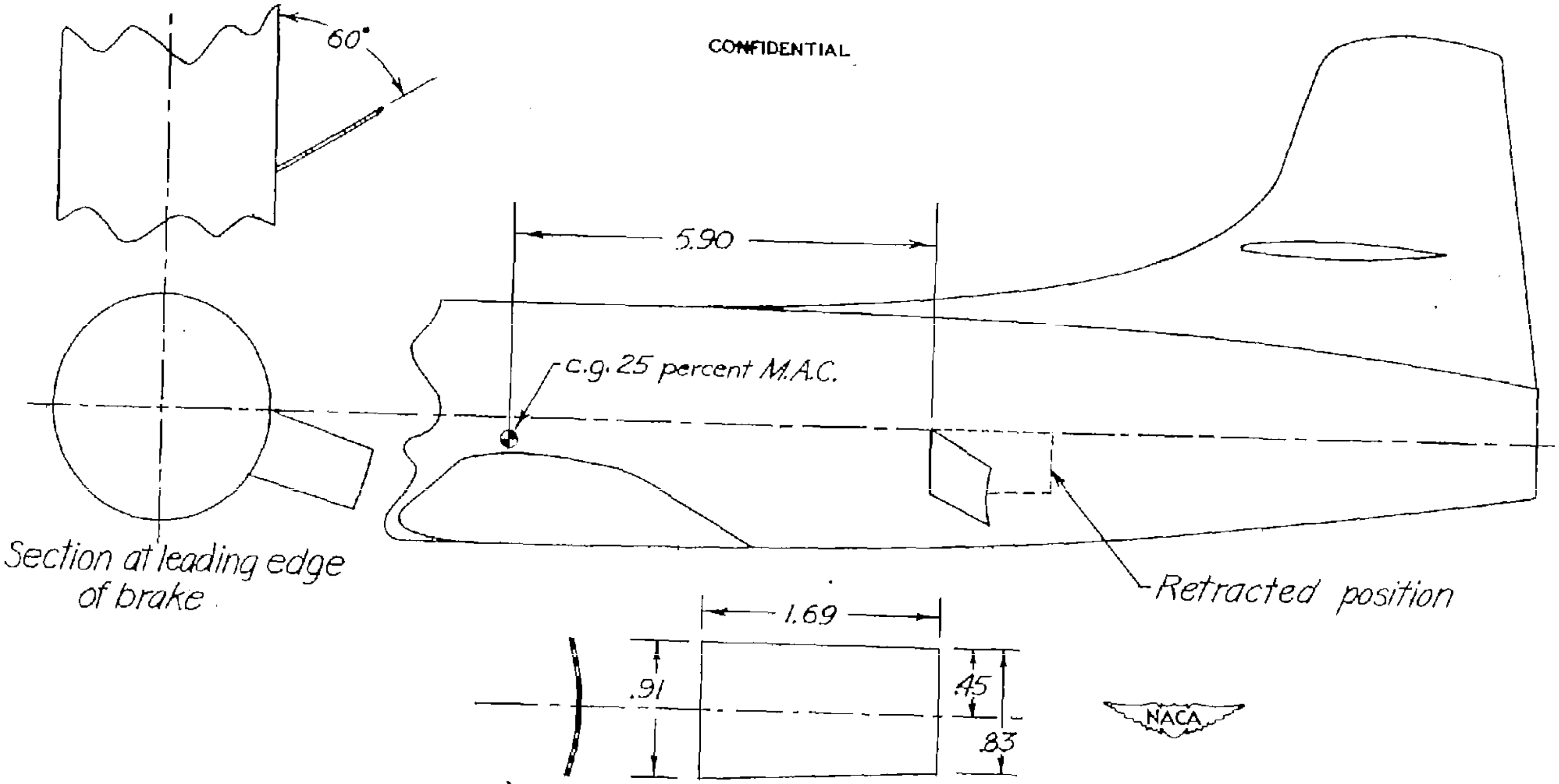

CONFIDENTIAL

Figure 2.–Speed-reduction brakes on D-558-I model. All dimensions in inches.

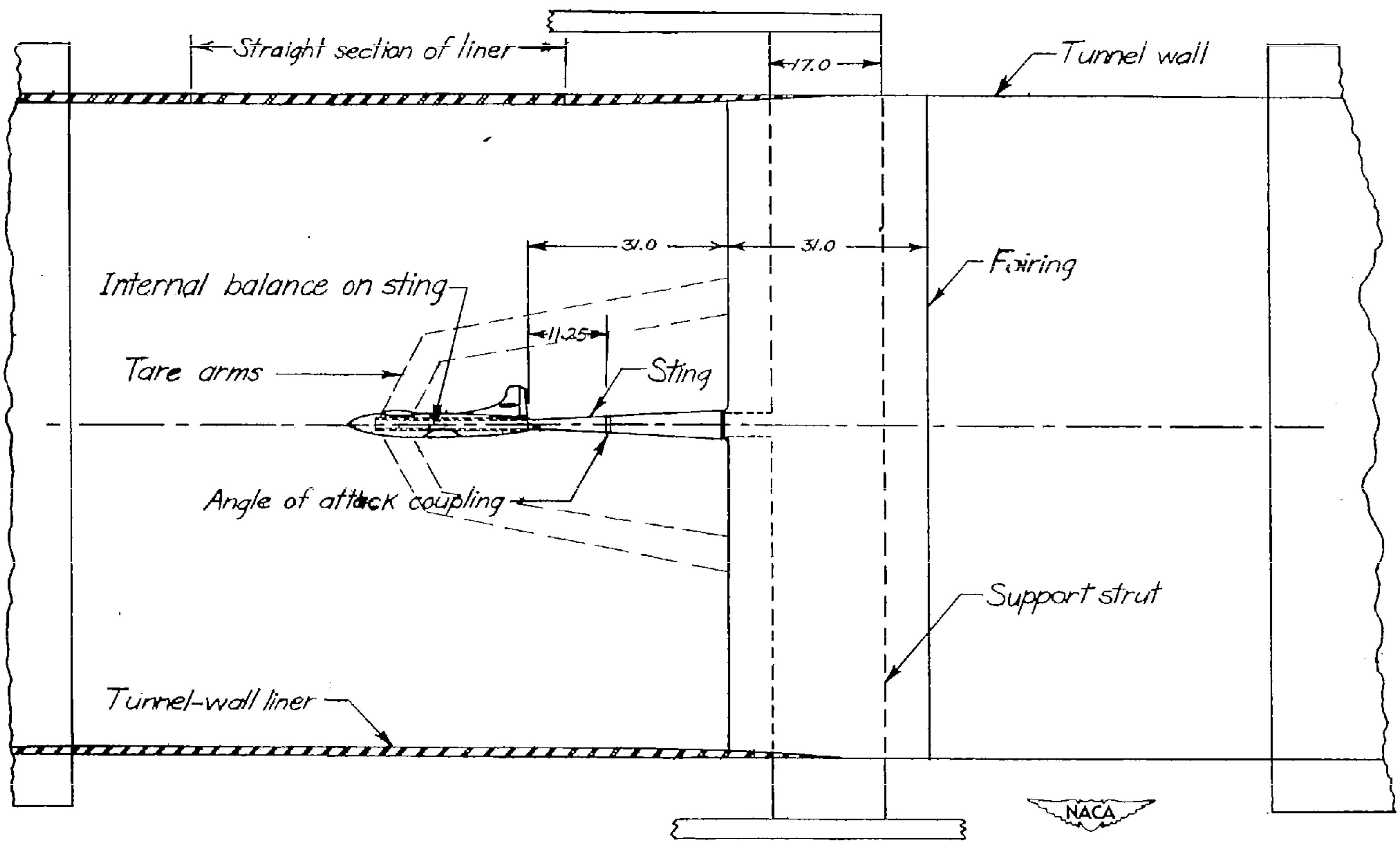

Figure 3 .- Model on sting support in the Langley 8-foot high-speed tunnel All dimensions in inches.

CONFIDENTIAL

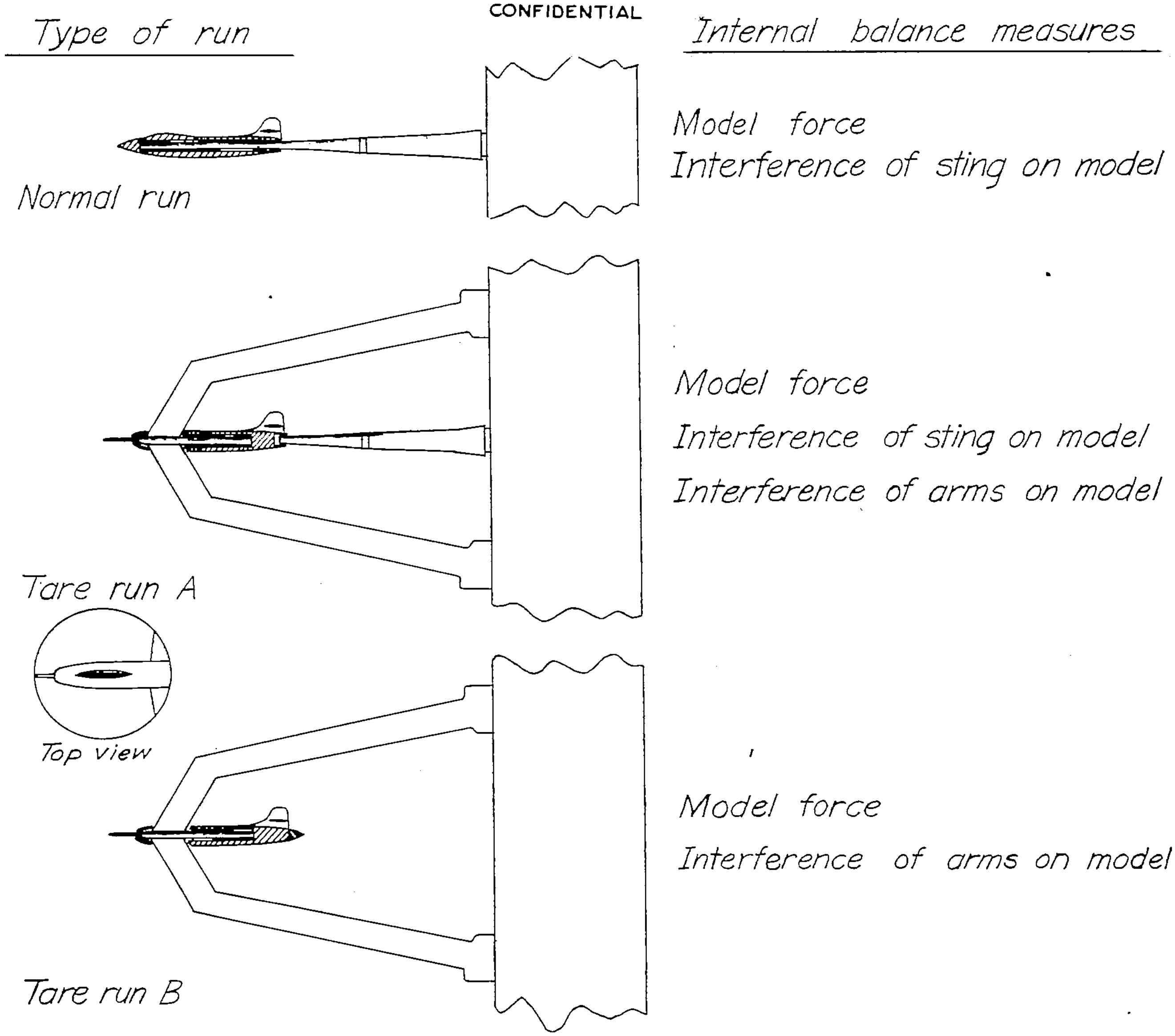

Tare run A – Tare run B = Interference of sting on model

Normal run – (A-B) = Model force

CONFIDENTIAL

Figure 4.—Model setups and tare evaluation technique.

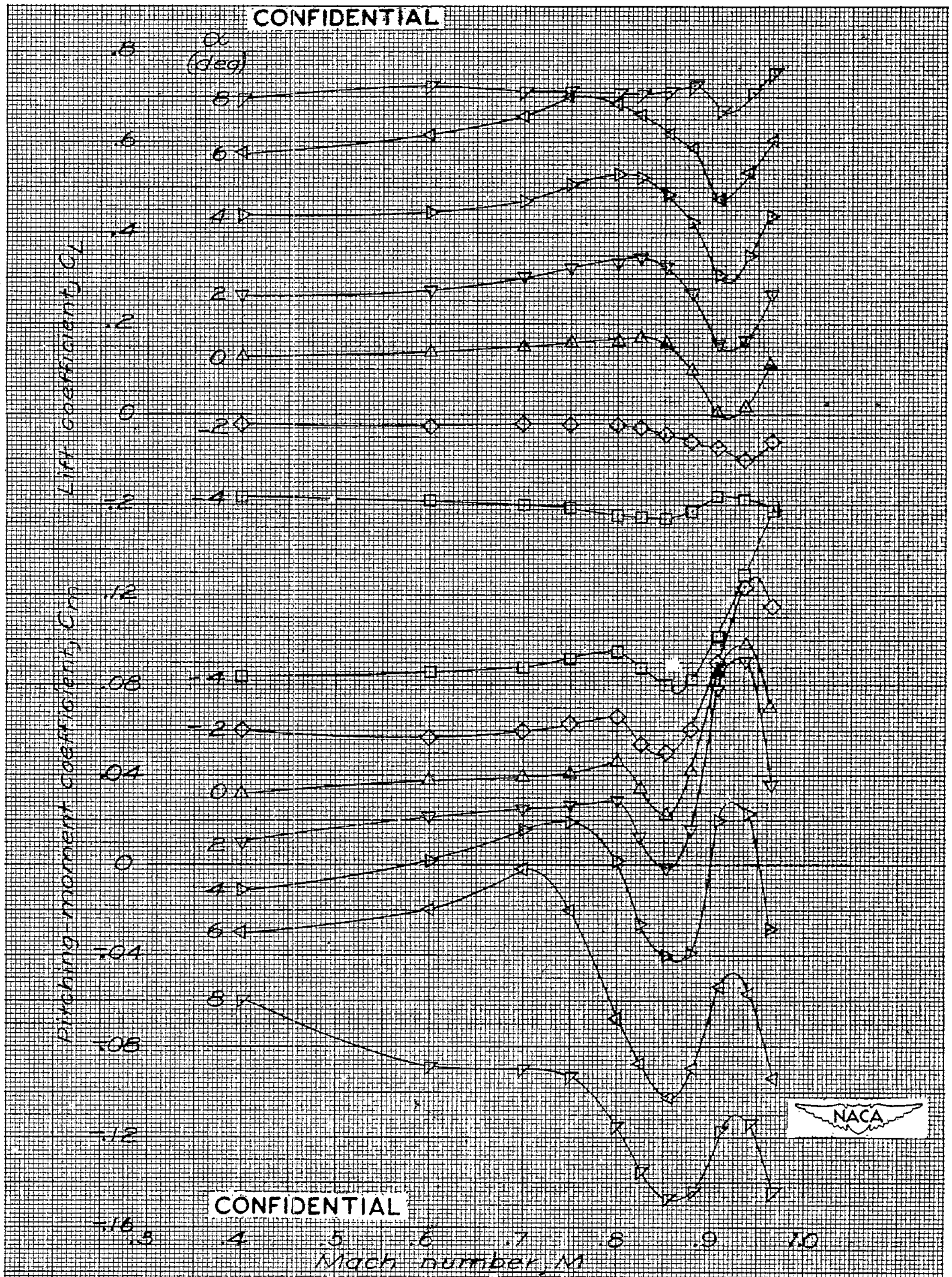

Figure 5.— Variation of lift coefficient and pitching-moment coefficient with Mach number for various angles of attack. Complete model with speed-reduction brakes; $i_t = 2.2°$; $\delta_e = 0°$.

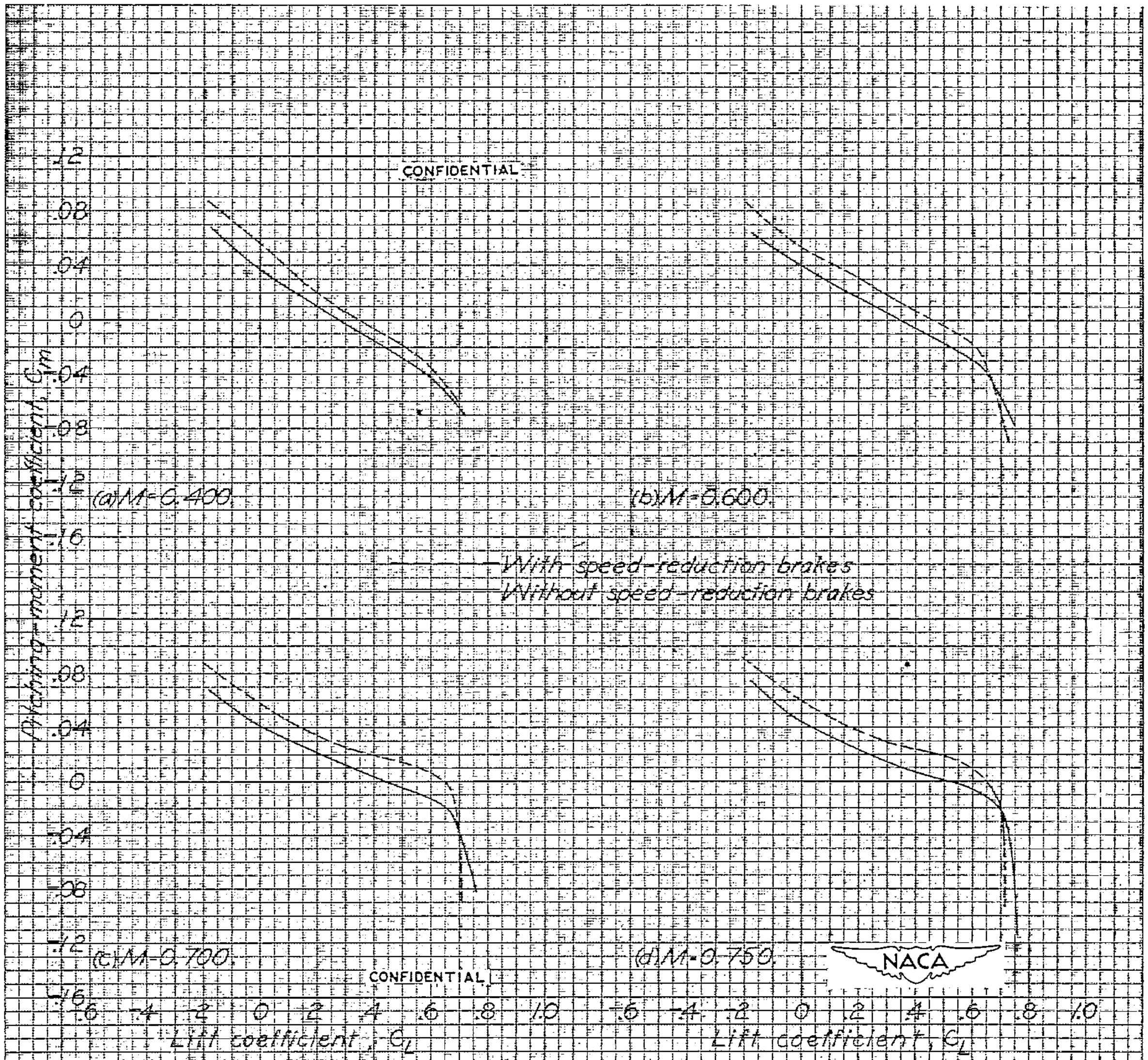

Figure 6.– Variation of pitching-moment coefficient with lift coefficient for various Mach numbers. Complete model with and without speed-reduction brakes; $i_t = 2.2^\circ$; $\delta_e = 0^\circ$.

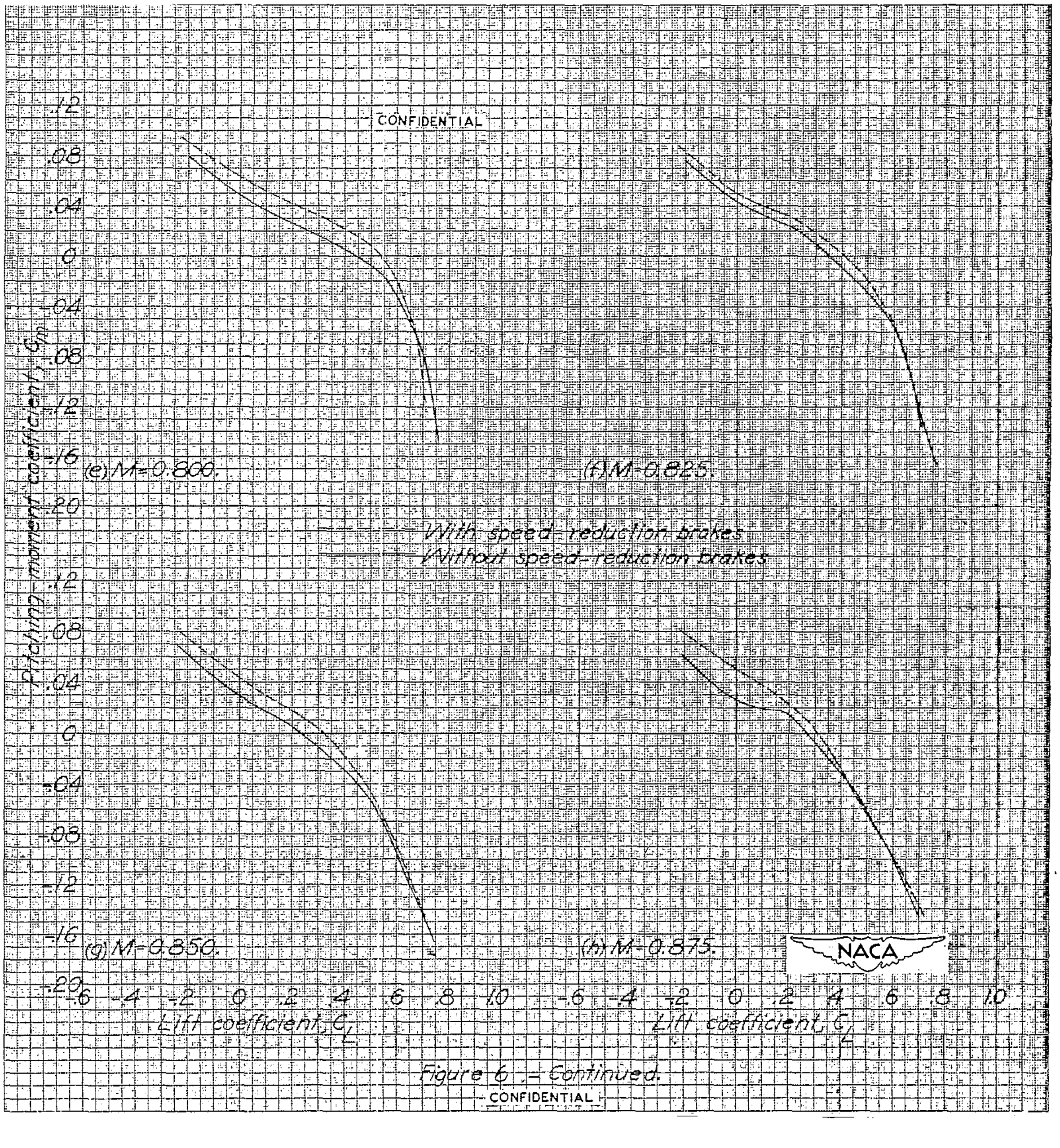

Figure 6.- Continued.

CONFIDENTIAL

CONFIDENTIAL

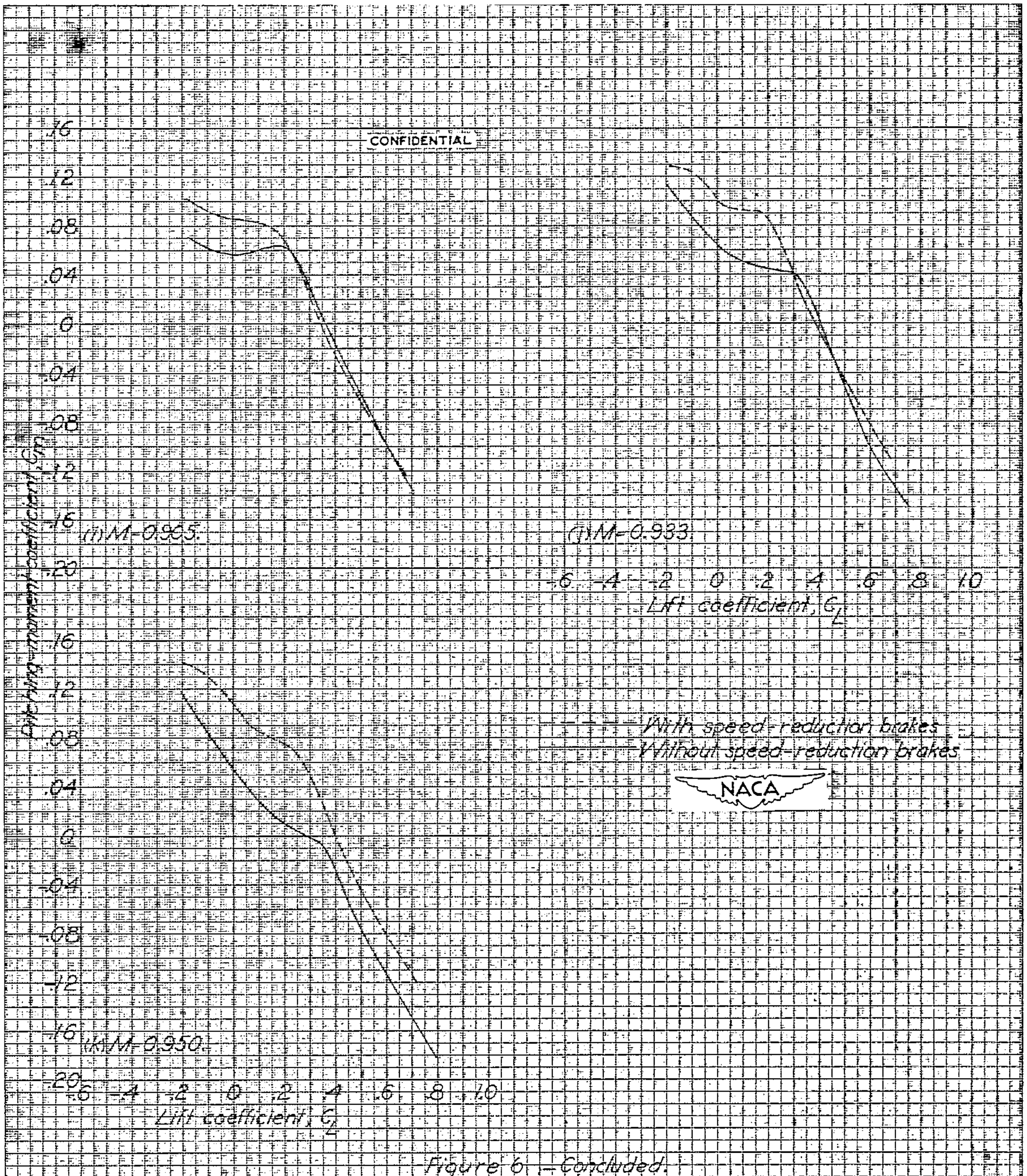

Figure 6.- Concluded.

CONFIDENTIAL

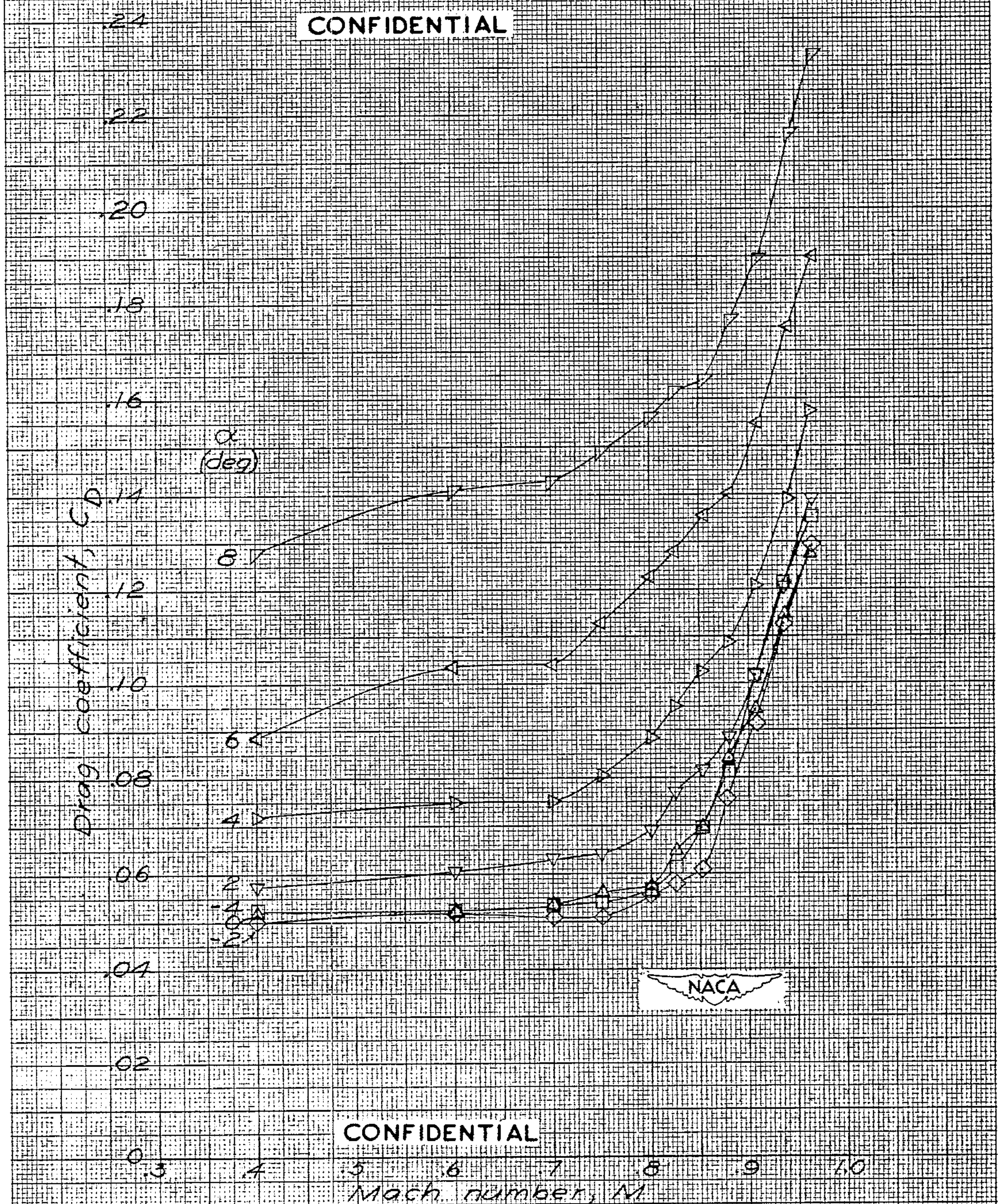

Figure 7.- Variation of drag coefficient with Mach number for various angles of attack. Complete model with speed-reduction brakes; $i_t = 2.2°$; $\delta_e = 0°$.

CONFIDENTIAL

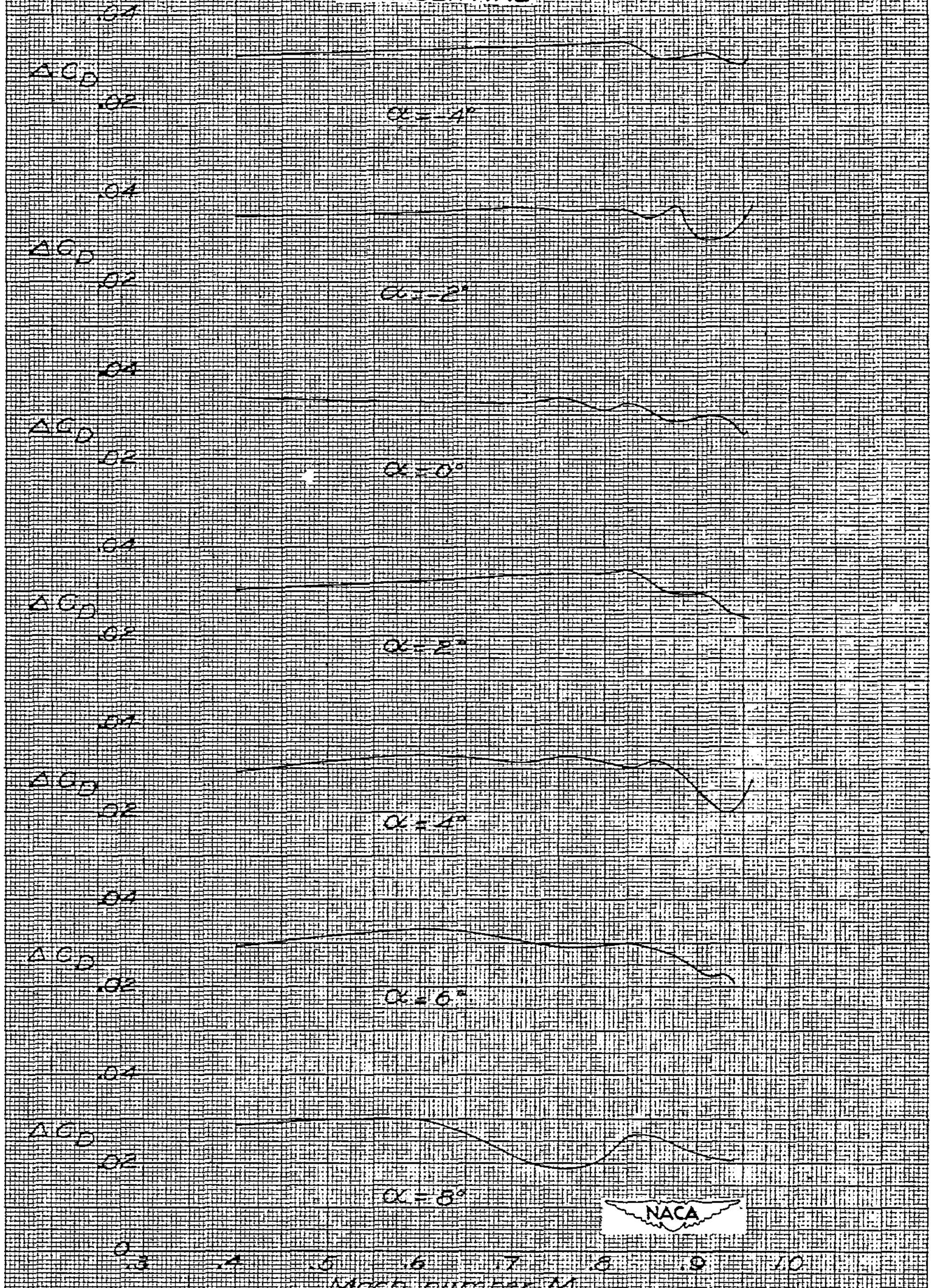

Figure 6.- Variation of drag-coefficient increment ΔC_D due to speed-reduction brakes with Mach number for various angles of attack. Complete model; $i_t = 2.2°$; $\delta_e = 0°$.

CONFIDENTIAL

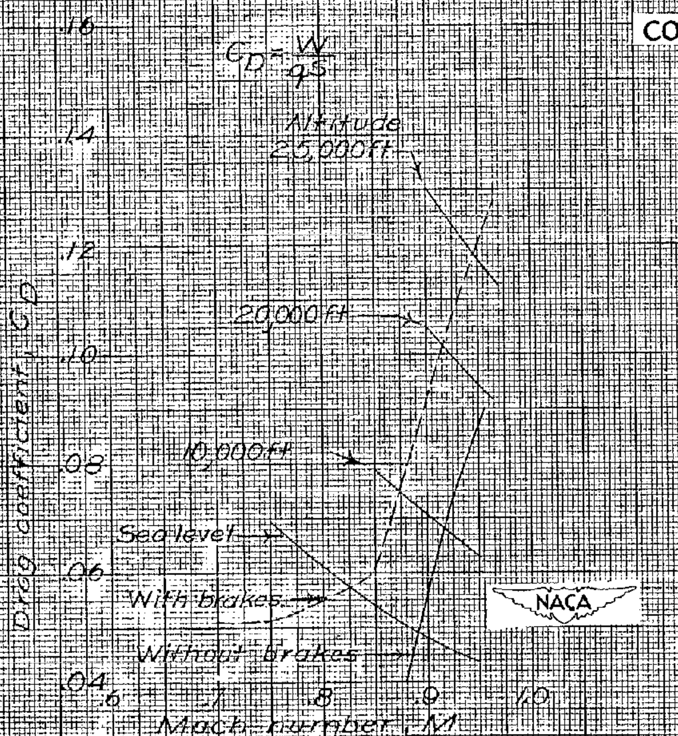

Figure 9.– Variation of drag coefficient for $C_L=0$ with Mach number for terminal Mach number prediction. Complete model; $i_t=2.2°$; $\delta_e=0°$, with and without speed-reduction brakes.

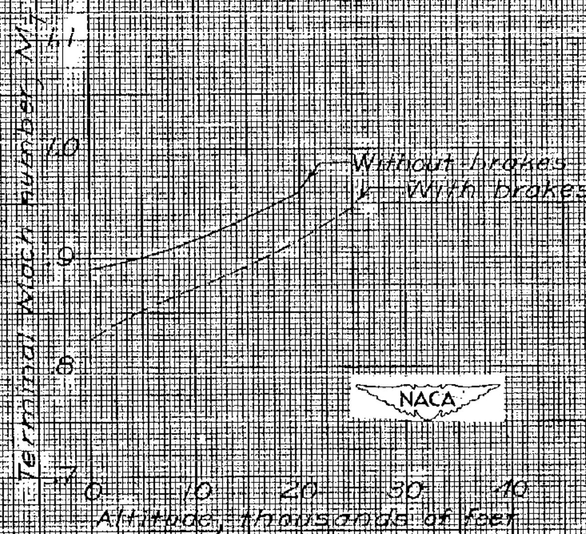

Figure 10.– Variation of terminal Mach number with altitude, with and without speed-reduction brakes.

CONFIDENTIAL

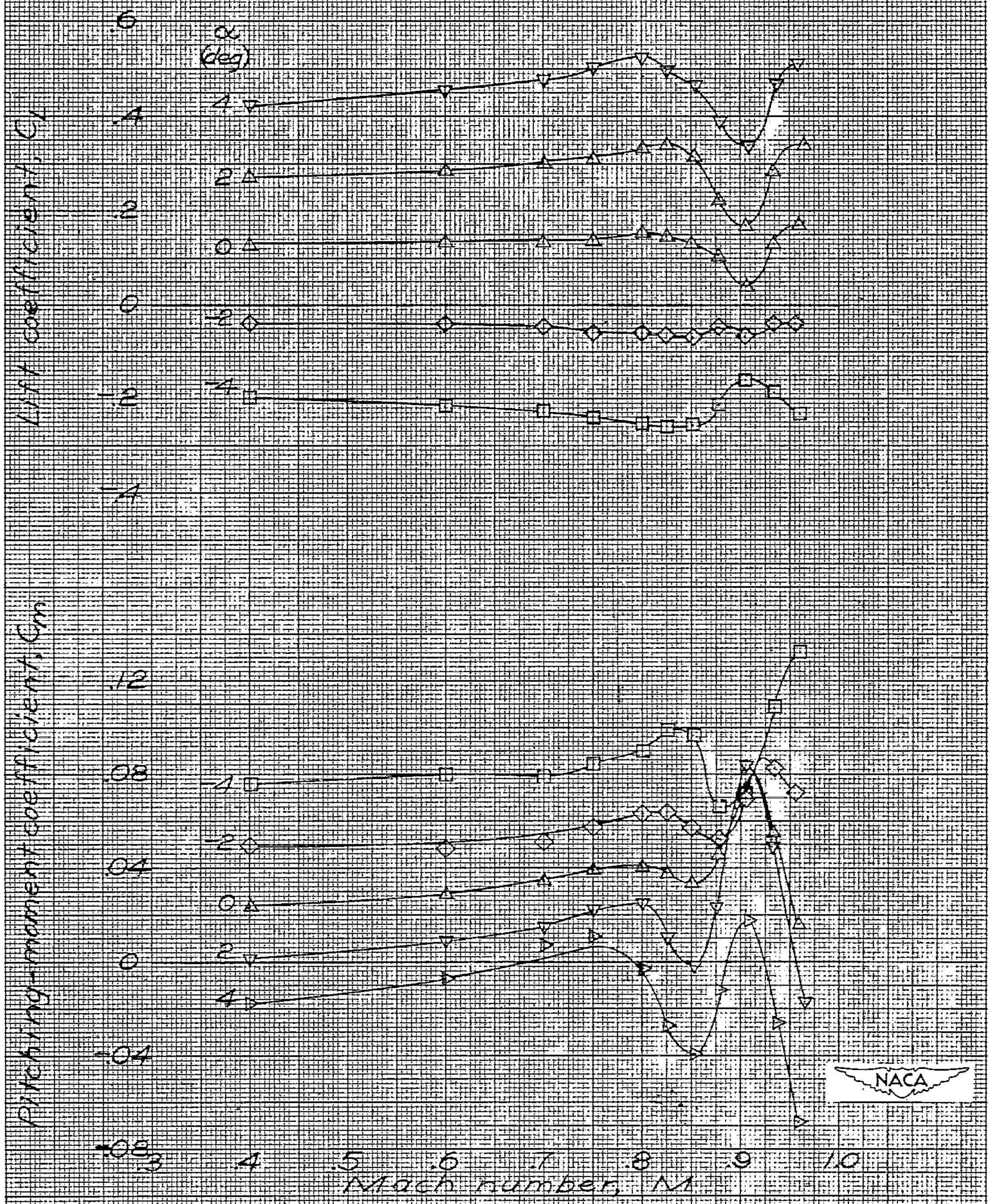

Figure 11.- Variation of lift coefficient and pitching-moment coefficient with Mach number for various angles of attack. Complete model; $i_t = 2.2°$; $\delta_e = 0°$; NACA 65-010 wing.

CONFIDENTIAL

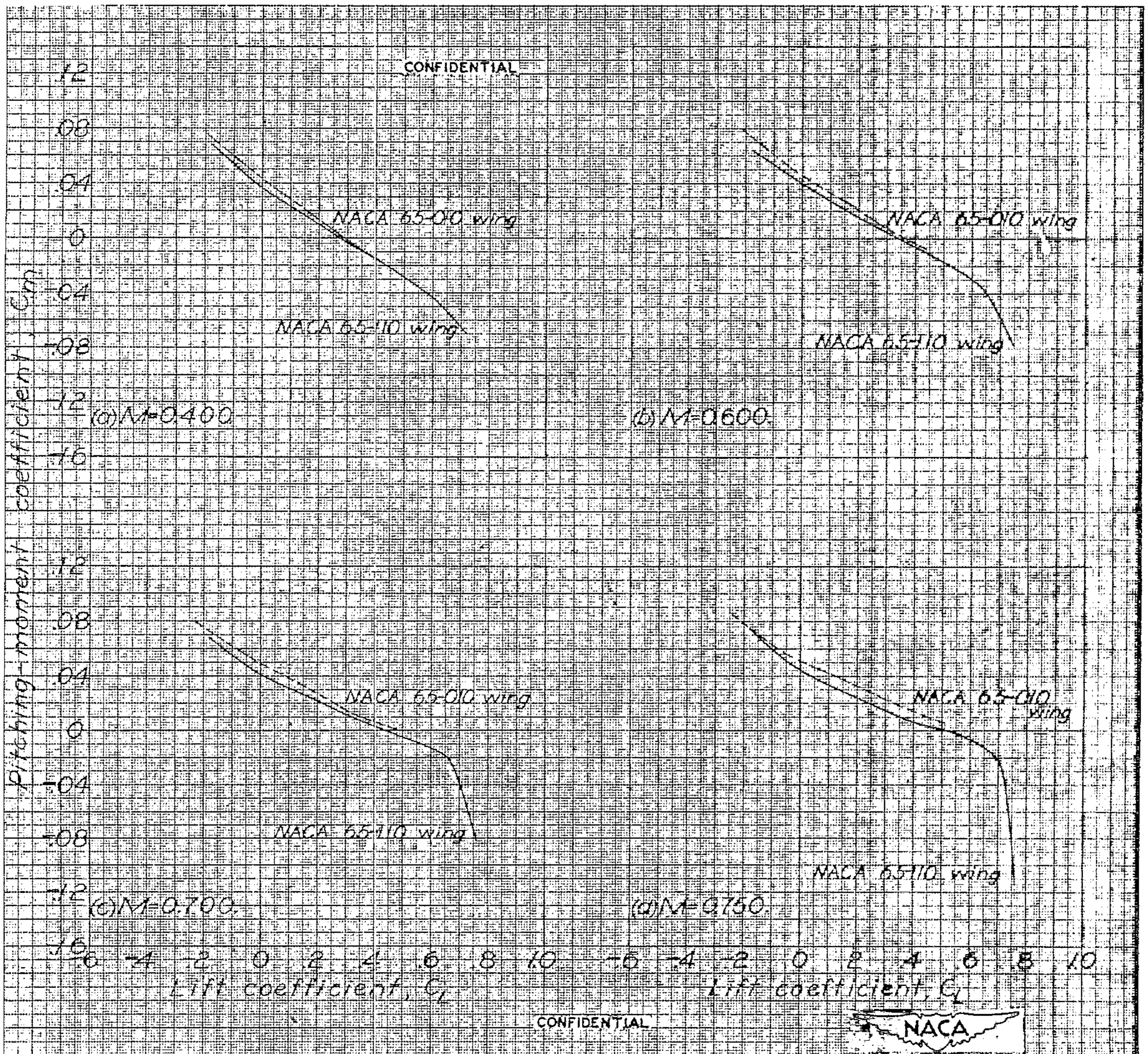

Figure 12.— Variation of pitching-moment coefficient with lift coefficient for various Mach numbers. Complete model, $i_t = 2.2°$; $\delta_e = 0°$; NACA wings 65-110 and 65-010.

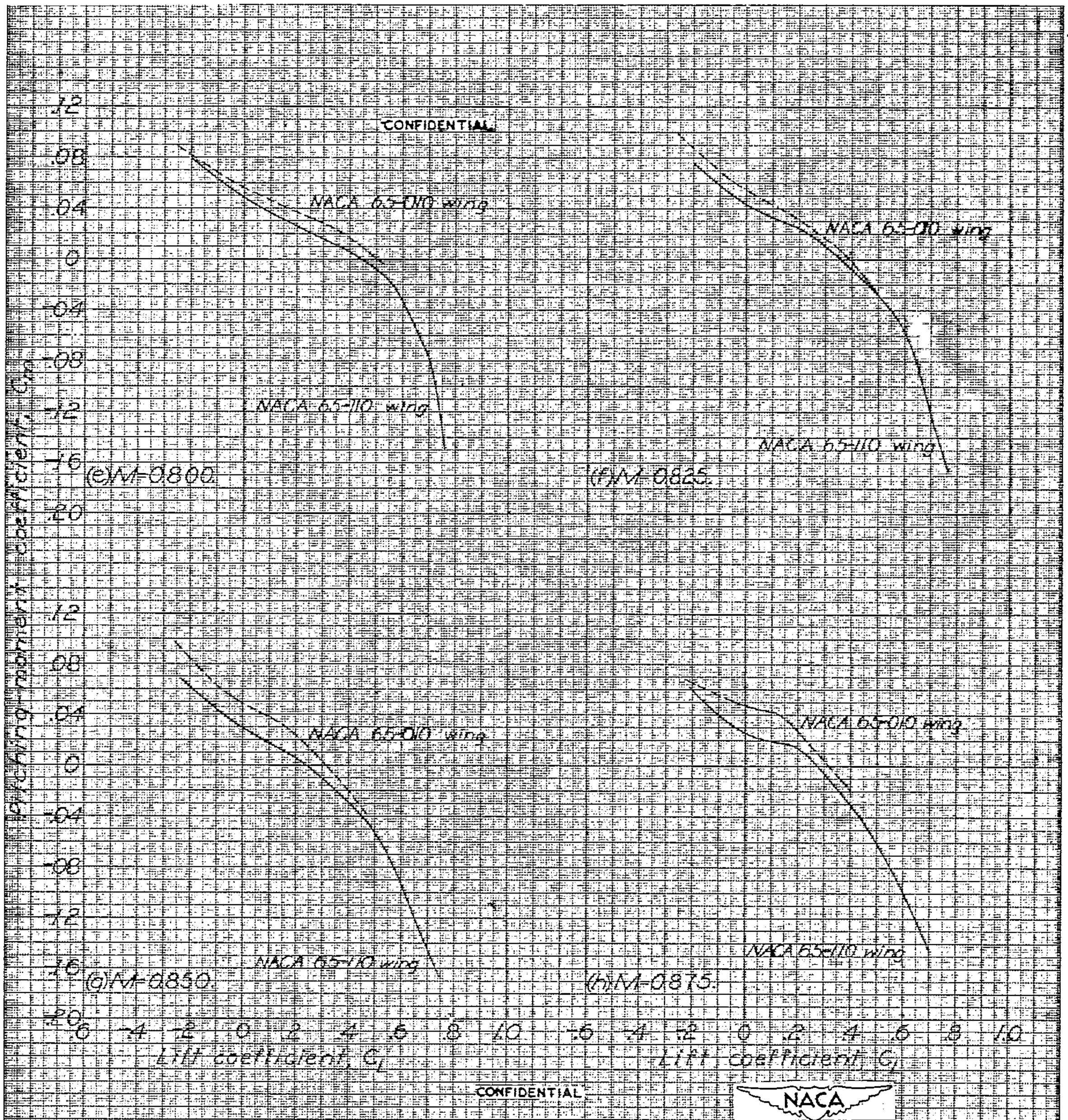

Figure 12.— Continued.

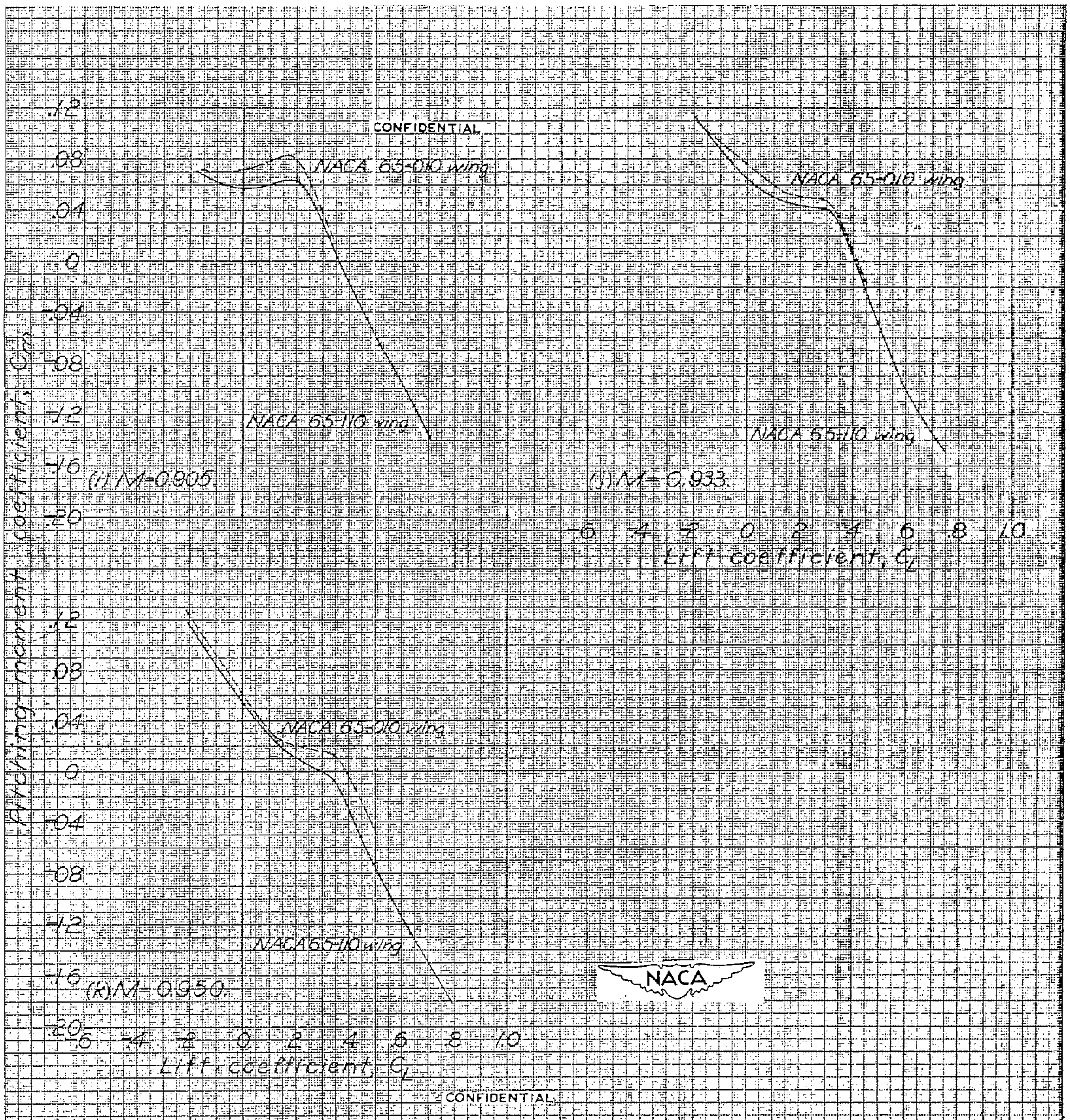

Figure 12.— Concluded.